

mass spectrometer located ≈ 8 cm from the nozzle tip. The photoionization wavelength resolution used is 1.5 Å [full width at half-maximum (FWHM)].

Figure 1a shows the temporal profile of the CH_3SCH_3 beam pulse observed by photoionization at 1280 Å using a multichannel scaler with a channel width of 10 μs . Time zero of the spectrum corresponds to the initiation of the trigger pulse for opening the pulse valve. The triggering pulse for firing the excimer laser is delayed by 500 μs with respect to time zero.²⁵ The temporal profiles for the CH_3S and CH_3 beam pulses observed at 1250 Å and laser pulse energies of 60 and 35 mJ are shown in Figure 1b,c, respectively. The accumulation time for each spectrum is 5 min. The vertical scale indicates the actual counts of various channels. The peaks indicated by arrows in Figure 1b,c are identified as background ions caused by the excimer laser alone.²⁶ In order to avoid the background due to the excimer laser, the CH_3S^+ (CH_3^+) ion counts resulting from photoionization of CH_3S (CH_3) radicals are measured by gating the scaler in the temporal range of 0.9–2.9 ms.

The observed widths [≈ 800 μs (FWHM)] of the CH_3S and CH_3 beam pulses are lower than that [≈ 1500 μs (FWHM)] of the CH_3SCH_3 beam pulse, but are greater than that expected based on the spatial distribution (≈ 6 mm) of the photodissociation region and the laser pulse width [≈ 8 ns (FWHM)]. Since the radicals initially formed by photodissociation have substantial kinetic energies, the greater than expected width may be attributed to the expansion effect of translationally hot radicals and to their collisions with Ar and CH_3SCH_3 molecules in the free jet. This interpretation implies that the density of the free jet has to be sufficiently high and the pulse width sufficiently wide for complete trapping and cooling of the internally and translationally hot radicals produced by photodissociation. With use of similar experimental procedures and conditions, photoionization efficiency (PIE) spectra for SO^{27} and CS^{28} prepared by 193-nm laser photodissociation^{29,30} of SO_2 and CS_2 , respectively, show that SO and CS sampled at the photoionization region are in the $v = 0$ states.

The PIE spectra for CH_3S^+ from CH_3S and for CH_3S^+ from CH_3SCH_3 in the ranges of 1200–1470 and 1020–1150 Å are depicted in Figure 2. The threshold for the formation of CH_3S^+ (or CH_2SH^+) from CH_3SCH_3 is determined to be ≈ 1049 Å.^{16,31,32} Therefore, the CH_3S^+ ions observed at wavelengths > 1200 Å are due to the photoionization of CH_3S . The PIE spectra for CH_3^+ from CH_3 and for S^+ from S^{33} near their thresholds are also shown in the figure. The observed IEs of CH_3 and S are consistent with the literature values.^{34,35} Since the photoionization of CH_3S involves the removal of an essentially nonbonding electron from S , the IE of CH_3S is expected to be sharp. As the photon energy is increased, the PIE for CH_3S^+ is found to rise rapidly from 1344

± 2 Å, which is interpreted as the IE for CH_3S to form **2**. On the basis of the energy release measurements, $\Delta H_{\text{f}}(\text{CH}_3\text{S})$ is determined to be 35.0 ± 1.0 kcal/mol.^{16,36} Most recently, a value $\Delta H_{\text{f}}(\text{CH}_3\text{S}) = 31.4 \pm 0.5$ kcal/mol has been obtained by Wine and co-workers³⁷ using a chemical kinetics bromination method. These values, together with the IE for CH_3S to **2**, yield a value of 244.1–247.7 kcal/mol for $\Delta H_{\text{f}}(\text{CH}_3\text{S}^+)$. The literature value for $\Delta H_{\text{f}}(\text{CH}_2\text{SH}^+)$ is in the range of 206–209 kcal/mol.^{4,9,16} The finding that $\Delta H_{\text{f}}(\text{CH}_3\text{S}^+)$ is greater than $\Delta H_{\text{f}}(\text{CH}_2\text{SH}^+)$ by 35–42 kcal/mol is consistent with the theoretical prediction of > 27 kcal/mol.¹⁷ The PIE of CH_3S in the range of 1344–1470 Å is small and decreases slowly toward lower photon energy, indicating that the Franck-Condon factor for photoionization to **1** is unfavorable.

(36) On the basis of energy release measurements of the processes, $\text{CH}_3\text{SSCH}_3 + h\nu(193 \text{ nm}) \rightarrow 2\text{CH}_3\text{S}$, $\text{CH}_3\text{SCH}_3 + h\nu(193 \text{ nm}) \rightarrow \text{CH}_3\text{S} + \text{CH}_3$, and $\text{CH}_3\text{SH} + h\nu(193 \text{ nm}) \rightarrow \text{CH}_3\text{S} + \text{H}$. See ref 16.

(37) Nicovich, J. M.; Kreutter, K. D.; van Dijk, C. A.; Wine, P. H. Private communication.

Distorted Amides: Correlation of Their Enhanced Solvolysis with Local Charge Depletions at the Carbonyl Carbon

K. E. Laidig*[†] and R. F. W. Bader

Department of Chemistry, McMaster University
Hamilton, Ontario L8S 4M1, Canada

Received July 26, 1990

Recently, Bennet et al. studied a series of tertiary amides in which the rate of base hydrolysis was compared with structural characteristics determined by X-ray diffraction.¹ They observed that distortion of the amide group away from planarity led to enhanced rates of hydrolysis. The distortion, resulting in the pyramidalization of the amide nitrogen, is obtained by rotation about the C–N bond. The hydrolysis rates demonstrated that the greater the distortion, the greater the susceptibility of the carbonyl carbon to attack. The geometric observations agree with theoretical predictions which demonstrated that the resonance model fails to satisfactorily predict the consequences of rotation about the C–N bond.² This leaves open the origin of the enhanced rate of hydrolysis in the apparent absence of an accompanying loss in amidic resonance.

The Laplacian of the electronic charge density ($\nabla^2\rho$) predicts the sites of electrophilic and nucleophilic attack, as well as their relative propensity toward reaction,³ the structures and geometries of hydrogen-bonded complexes,⁴ the directing abilities of substituents in aromatic electrophilic substitution,⁵ the relative susceptibility of activated double bonds to Michael addition,⁶ and the relative kinetic reactivity of the syn and anti faces of the carboxylate anion.⁷ This note presents such a study of the relative reactivities of planar and pyramidalized formamide to nucleophilic attack by comparing the relative magnitudes of $\nabla^2\rho$ at the critical points in the valence-shell charge concentration (VSCC) of the carbonyl carbon. These are the holes in the VSCC which locate the sites of local charge depletion ($\nabla^2\rho > 0$), the predicted sites for nucleophilic attack.³ These predictions, together with the predicted direction of approach of the nucleophile, agree with both experiment^{8a} and theory.^{8b}

[†] Present address: University Chemical Laboratory, Lensfield Road, Cambridge CB2 1EW, U.K.

(1) Bennet, A. J.; Wang, Q. P.; Slebocka-Tilk, H.; Somayaji, V.; Brown, R. S.; Santarsiero, B. D. *J. Am. Chem. Soc.* **1990**, *112*, 6383.

(2) Wiberg, K. B.; Laidig, K. E. *J. Am. Chem. Soc.* **1987**, *109*, 5953.

(3) (a) Bader, R. F. W.; MacDougall, P. J.; Lau, C. D. H. *J. Am. Chem. Soc.* **1984**, *106*, 1594. (b) Bader, R. F. W.; MacDougall, P. J. *J. Am. Chem. Soc.* **1985**, *107*, 6788.

(4) Carroll, M. T.; Chang, C.; Bader, R. F. W. *Mol. Phys.* **1988**, *63*, 387.

(5) Bader, R. F. W.; Chang, C. *J. Phys. Chem.* **1989**, *93*, 2946.

(6) Carroll, M. T.; Cheeseman, J. R.; Osman, R.; Weinstein, H. *J. Phys. Chem.* **1989**, *93*, 5120.

(7) Laidig, K. E. *J. Am. Chem. Soc.*, submitted.

(25) The excimer laser delay time is chosen to maximize the CH_3S signal as observed by photoionization.

(26) These peaks are the only features in the spectra when the photoionization vacuum UV light source is off.

(27) Norwood, K.; Nourbakhsh, S.; He, G.-Z.; Ng, C. Y. Unpublished results.

(28) Norwood, K.; Nourbakhsh, S.; He, G.-Z.; Ng, C. Y. *Chem. Phys. Lett.*, submitted for publication.

(29) The 193-nm laser photofragmentation TOF mass spectrometric study of SO_2 shows that the vibrational distribution of SO for $v = 0, 1, 2$, and 3 is 0.05:0.23:0.67:0.05. See: Felder, P.; Effenhauser, C. S.; Haas, B. M.; Huber, J. R. *Chem. Phys. Lett.* **1988**, *148*, 417.

(30) It is known that CS formed in 193-nm laser photofragmentation of CS_2 are in the $\text{CS}(X, v=0-13)$ states, corresponding to internal excitations up to 45 kcal/mol. See: Tzeng, W. B.; Yin, H.-M.; Leung, W.-Y.; Luo, J.-Y.; Nourbakhsh, S.; Flesch, G. D.; Ng, C. Y. *J. Chem. Phys.* **1988**, *88*, 1658 and references cited therein.

(31) The theoretical study of Radom and co-workers suggests that the singlet $\text{CH}_2=\text{SH}^+(^1A')$ is formed exclusively at the dissociation threshold from $\text{CH}_3\text{SCH}_3^+$ and $\text{CH}_3\text{SSCH}_3^+$. See ref 17.

(32) Akopyan, M. E.; Sergeev, Yu. L.; Vilesov, F. I. *Khim. Vys. Energ.* **1970**, *4*, 305.

(33) Sulfur atoms are produced from the 193-nm photodissociation of CH_3S . See ref 16.

(34) Chupka, W. A.; Lifshitz, C. *J. Chem. Phys.* **1968**, *48*, 1109.

(35) Lias, S. G.; Bartmess, J. E.; Liebman, J. F.; Homes, J. L.; Levin, R. D.; Mallard, W. G. *J. Phys. Chem. Ref. Data* **1988**, *17* (Suppl. 1), 68, 641.

Table I. Properties of Atoms and Critical Points in Formamide Structures

	ΔE , kcal/mol	r_{CN} , au	r_{CO} , au	$\nabla^2\rho$			θ , ^a deg	$d(\text{h1}-\text{ncc})$, ^b au	ϕ , ^c deg	$q(\text{C})$, ^d electrons	τ , ^e deg
				h1, au $\times 10^3$	h2, au $\times 10^3$	ncc, au $\times 10^3$					
1	0.0	2.548	2.255	130	130	-214	0.0	2.3	14	1.978	94.1
2	3.1	2.588	2.247	152	116	-270	6.0	2.4	30	1.936	106.6
3	7.6	2.616	2.242	153	114	-285	7.4	2.5	46	1.902	110.3
4	18.7	2.686	2.228	128	128	-332	0.0	3.0	109	1.777	110.8

^aThe angle the carbonyl H makes with the OCN plane. ^bThe distance between h1 and ncc. ^cThe torsion angle between h1 and ncc along the C-N bond. ^dThe net charge on the carbonyl carbon. ^eThe nitrogen pyramidalization angle, ncc-N-H.

The SCF calculations were done at the HF/6-31G**//HF/6-31G** level.⁹ We optimized the planar equilibrium structure, **1**, the structure corresponding to the transition state for internal rotation,² which maximizes the pyramidalization of the nitrogen, **4**, and two distorted geometries with fixed O-C-N-H torsional angles of 40° and 60°, **2** and **3**, respectively (Figure 1).

The Laplacian quantitatively determines the extent of pyramidalization of N during C-N bond rotation. The charge concentrations of the Laplacian ($\nabla^2\rho < 0$) are the physical analogues of Lewis electron pairs.^{3,10} Thus the VSCC of the pyramidalized N in **4** exhibits three bonded and one nonbonded charge concentrations, approximately tetrahedrally directed. In **1** the nonbonded charge concentration (ncc, Table I) on N is necessarily present as two equivalent maxima, above and below the plane. The VSCCs of N in **2** and **3** already exhibit the tetrahedral structure found in **4**.

Rotation about the C-N bond also results in slight pyramidalization of the carbon. This enlarges the hole (i.e., increases the value of $\nabla^2\rho$ at the critical point), h1, occupying the tetrahedral position in the VSCC of the carbonyl carbon. This is the origin of enhanced susceptibility in distorted amides, the greater depletion of charge at the hole in the carbon's VSCC. This prediction of increased susceptibility to nucleophilic attack is made quantitative by the values of $\nabla^2\rho$. The holes in the VSCC of structures **2** and **3** display different reactivities. The one syn to the amide hydrogens and interior to the pyramid, h2, is less positive and hence less reactive than are the corresponding critical points in the planar amide while the enlarged hole on the opposing face, h1, is more positive and more reactive. The distance between h1 and ncc and their associated torsion angle ϕ across the C-N bond increase with increased rotation about the C-N bond.

The relative location of a critical point predicts the angle of nucleophilic attack.³⁻⁶ The critical points denoting the holes of the carbonyl carbon are found ~ 0.53 Å from its nucleus (Figure 1). In the planar amide each forms an angle of 109° with the C-O bond, increasing to a maximum of 112° in **3**, in agreement with experiment.⁸ The net charges on the carbonyl carbon atoms are determined by spatial integration of the charge density over the atomic basins (Table I). The pyramidalization of N changes its hybridization from sp^2 to sp^3 , resulting in the transfer of electronic charge from N to C, decreasing somewhat the large net positive charge on C. The distortion found in **2** is predicted to significantly increase the reactivity of the carbonyl carbon in spite of a slight decrease in its net charge. This demonstrates that the dominant factor in determining relative reactivity is not the magnitude of an atomic charge but rather the extent of charge concentration or charge depletion, as determined by the Laplacian of the density.³⁻⁷

Our predictions of increased propensity for reaction are the result of the response of the VSCC to the geometric distortion about the carbonyl carbon. This reorganization of charge will occur in solution as well as in the gas phase. The field generated

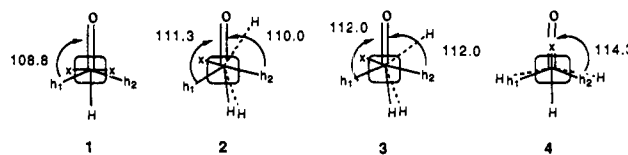


Figure 1. Newman projections of the four rotamers of formamide. Here h1 and h2 represent the more and less reactive holes in the VSCC of carbon, respectively, and x represents the ncc on nitrogen. The dashed lines to H represent the N-H bonds.

by solvent molecules might make a small perturbation to the VSCC, but previous experience with electric fields has shown that the greatest perturbations are made to the outer, diffuse distribution.^{11a} The VSCC, a tightly bound region of charge, is much less likely to be affected by external fields. This will be considered in detail in a future publication.^{11b}

The barrier to amidic rotation and its associated bond lengthening results from the transfer of charge from N to C, induced by the accompanying pyramidalization of N, which decreases the electron-nuclear attractive energy more than it decreases the repulsive energies.¹² Bennet et al.¹ explain the enhanced reactivity of the distorted amides by arguing that since N is pyramidalized in the transition state, the more distorted amide is closer in energy to the transition state. The present results show that this investment in energy also pyramidalizes the carbon, increasing the extent of its charge depletion, thereby increasing its susceptibility to nucleophilic attack.

(11) (a) Laidig, K. E.; Bader, R. F. W. *J. Chem. Phys.* **1990**, *93*, 7213. (b) Laidig, K. E., work in final preparation.

(12) Bader, R. F. W.; Cheeseman, J. R.; Laidig, K. E.; Wiberg, K. B.; Breneman, C. M. *J. Am. Chem. Soc.* **1990**, *112*, 6530.

Facile Aryl-Aryl Exchange between the Palladium Center and Phosphine Ligands in Palladium(II) Complexes

Kwang-Cheng Kong and Chien-Hong Cheng*

Department of Chemistry, National Tsing Hua University
Hsinchu, Taiwan 300, Republic of China
Received April 10, 1991

It is known that $\text{PdL}_2(\text{Ar})\text{X}$ (**1** (L = phosphine, Ar = aryl)) is involved as an important intermediate in a vast number of palladium-mediated organic syntheses such as carbonylation of aromatic halides,¹ arylation of olefins,² and coupling of aryl halides

(8) (a) Burgi, H. B.; Dunitz, J. D. *Acc. Chem. Res.* **1983**, *16*, 153. (b) Stone, A. J.; Erskine, R. W. *J. Am. Chem. Soc.* **1980**, *102*, 7185.

(9) (a) Hariharan, P. C.; Pople, J. A. *J. Chem. Phys. Lett.* **1972**, *66*, 217. (b) Hehre, W. J.; Ditchfield, R.; Pople, J. A. *J. Chem. Phys.* **1972**, *56*, 2257. (c) Binkley, J. S.; Pople, J. A. *J. Chem. Phys.* **1977**, *66*, 879. (d) Francl, M. M.; Pietro, W. J.; Hehre, W. J.; Binkley, J. S.; Gordon, M. S.; DeFrees, D. J.; Pople, J. A. *J. Chem. Phys.* **1982**, *77*, 3654.

(10) Bader, R. F. W.; Gillespie, R. J.; MacDougall, P. J. *From Atoms to Polymers*; Liebman, J. F., Greenberg, A., Eds.; VCH: New York, 1989.

(1) (a) Schoenberg, A.; Heck, R. F. *J. Am. Chem. Soc.* **1974**, *96*, 7761. (b) Yoshida, H.; Sugita, N.; Kudo, K.; Takezaki, Y. *Bull. Chem. Soc. Jpn.* **1976**, *49*, 1681. (c) Tanaka, M. *Tetrahedron Lett.* **1979**, 2601. (d) Heck, R. F. *Palladium Reagents in Organic Synthesis*; Academic Press: New York, 1985. (e) Bumagin, N. A.; Gulevich, Yu. V.; Beletskaya, I. P. *J. Organomet. Chem.* **1985**, *285*, 415.

(2) (a) Larock, R. C. *Pure Appl. Chem.* **1990**, *62*, 653. (b) Heck, R. F. *J. Am. Chem. Soc.* **1968**, *90*, 5518. (c) Heck, R. F. *J. Am. Chem. Soc.* **1968**, *90*, 5542. (d) Li, C. S.; Cheng, C. H.; Cheng, S. S.; Shaw, J. S. *J. Chem. Soc., Chem. Commun.* **1990**, 1774. (e) Li, C. S.; Cheng, C. H.; Liao, F. L.; Wang, S. L. *J. Chem. Soc., Chem. Commun.*, in press.